

# Design, Specification and Instalation of a Resistive Load Bank for a Hybrid-Electric Propulsion Test Bench<sup>\*</sup>

Daniel M. Esther<sup>\*</sup> Daniel de A. Fernandes<sup>\*\*</sup> Manuel A. Rendón<sup>\*\*\*</sup>

<sup>\*</sup> *Universidade Federal de Juiz de Fora (UFJF), Juiz de Fora, MG,  
(e-mail: daniel.miranda@engenharia.ufjf.br).*

<sup>\*\*</sup> *Universidade Federal de Juiz de Fora (UFJF), Juiz de Fora, MG,  
(e-mail: daniel.fernandes@ufjf.br)*

<sup>\*\*\*</sup> *Universidade Federal de Juiz de Fora (UFJF), Juiz de Fora, MG,  
(e-mail: manuel.rendon@ufjf.br)*

---

**Abstract:** The present work describes the design process, building and testing of an electronically-controlled resistive load bank for being used in a lab environment. The bank's basic characteristics are from a preliminary design on a previous work. The bank is part of an aircraft hybrid-electric propulsion test bench for stationary analysis, aiming to be low-cost and safe to handle. It is intended to simulate the variable mechanical load that an aircraft propeller applies to the drivetrain axis, at different rotation speeds on steady state conditions. Supplied by an electrical generator (EG), it can apply its resistive load in steps, which gets converted into a mechanical load by the generator. The support frame that houses the resistive elements and cooling fans was designed, built and assembled. Two sensor boards were developed to measure voltages and currents. The bank's controller is implemented with an *Arduino* board, employs a real-time operating system (RTOS) and communicates with a supervisory system hosted on a computer through a Controller Area Network (CAN) bus. The program's user interface was created as a Windows Forms App to allow ease of use and real-time monitoring of the bank's operation. A single load tap was built and tests were performed on it to validate sensor performance and acquire thermal response curves. Results indicate the system operates predictably and reliably, encouraging further developments.

*Keywords:* hybrid-electric propulsion, test bench, resistive load bank, real-time operating system.

---

## 1. INTRODUCTION

### 1.1 Context

The Hybrid-Electric Propulsion Laboratory (LAPHE), the first of its kind in the southern hemisphere, is a facility that supports multi-disciplinary research efforts in several engineering areas. A test bench for stationary testing of an aeronautical hybrid engine was assembled to carry out measurements, and validate several design developments. These works aim to evaluate the combined operation of the devices that compose the hybrid-electric system: Battery bank, power electronic converters (PECs), electric motors (EMs), internal combustion engines (ICEs), and propeller. However, rotational tests are usually hard to manage, and involve significant risks specially at high speeds. To overcome this a resistive load bank was designed to be connected to the output of an EG mounted on the axis, aiming to substitute the propeller. The torque applied by the EG on the axis emulates the mechanical load that would otherwise be applied by the propeller.

A previous work by Esther et al. (2020) proposes a preliminary design, states its main goals and lists components.

<sup>\*</sup> This work was possible due to funds from FAPEMIG and UFJF.

This paper describes the changes and improvements done to the original design, and presents a prototype that was assembled to validate performance.

### 1.2 Load Banks in Industry and Energy Research

Load banks are devices that apply an energy demand to a power source, simulating the load it would face on normal operation. They are used to test devices such as uninterruptible power supplies (UPSs), PECs, batteries, ICE-powered EGs, aircraft generators, among others (Simplex, 2020). For backup systems such as UPSs, performance tests are typically conducted regularly to ensure a proper generation operation when demanded (Worldwide Power Products, 2020; Bearn, 2012).

Experimental tests are required to characterize the load influence on motor performance. This evaluation is possible by employing resistive load banks, that might emulate the power demand through electrical blocks. A paper presented a 3.5kW resistive load bank to be applied in a test bench for a diesel ICE, coupled to an alternator, aiming to perform mechanical, thermal, and emissions studies. Power control circuits and safety devices were considered (Celis Quintero et al., 2020).

Equipment for testing PECs at high values of frequency, voltage, and power are usually not commercially available. Jackson et al. (2021) introduces a resistive load bank, able of supplying both DC and AC loads, and designed for testing high frequency inverters. It is computer-controlled, with load steps triggered at zero crossings.

Another work describes an inexpensive solution to absorb excess energy from photovoltaic (PV) panels in isolated microgrids, while maintaining a diesel ICE power source as a backup. It includes a resistive load bank for peak periods. A control algorithm was developed to monitor and control the grid's generation (Sepasi et al., 2023).

Raj et al. (2023) present an automated load bank design consisting of resistive, inductive and capacitive elements switched by contactors all inside a single enclosure; it employs an *ESP32* microcontroller and connects to an *Arduino* IoT Cloud.

Another paper (Prapurt and Lothongkam, 2022) presents a 20 kW resistive load bank for testing standby EGs, controlled by an *Arduino Mega* board. An AC voltage device using Silicon Controlled Rectifiers (SCRs) controls the load, which is composed of heater windings arranged in two parallel delta-connected three-phase taps. A single 4,500 cubic feet per meter (CFM) industrial fan cools the heater sets, which are fitted inside a rolling steel cart.

Kehler et al. (2013) studied and simulated an electronically adjustable, three-phase AC load. A Voltage Source Converter (VSC) and LCL filter couple the three-phase AC sources to a DC bus, and a Buck converter controls DC voltage and delivers power to a resistor. The VSC synthesizes sinusoidal currents and allows fine tuning of both active and reactive power draw.

### 1.3 Objective

The aim of this work is to refine, construct and test the original proposal (Esther et al., 2020), to describe the developments accomplished, and to evaluate whether the load bank is able to substitute the mechanical load of the propeller in the test bench.

The design aims to be used in academic and research environments, with relatively cheap and accessible components, and its modularity facilitates maintenance and allows scalability.

## 2. LOAD BANK DESCRIPTION

### 2.1 System Overview

The proposed load bank is meant to apply a resistive load to a three-phase electrical generator (EG), with nominal voltage of 380V according to values presented in Table 1.

Table 1. Electrical Characteristics

Parameter	Value	Unit
Operating Voltage	380/220	V
Frequency Range	60 - 600	Hz
Power per Tap	3.0	kW
Number of Taps	10	-
Nominal Power	30.0	kW

The bank can provide its load in steps by switching several parallel taps, connected by mechanical contactors to an internal three-phase 3-wire bus.

The actual components of the resistive load are commercial devices, more specifically, 127V 1000W replacement heating elements for hair dryers. They are cooled by 12V 0.56A fans that generate an airflow of up to 169 CFM.

The whole system is aimed to be managed by a controller that reads the signals from the sensors, sends switching signals to the taps, records each tap's total usage time and can perform basic fault detection and defective tap isolation. The controller communicates with a supervisory program through a Controller Area Network (CAN) bus, allowing the user to monitor its internal state and send load requests remotely.

### 2.2 Electric Circuit

The power circuit of the bank is presented in Figure 1, protected by a 63 A 3 kA thermomagnetic circuit breaker.

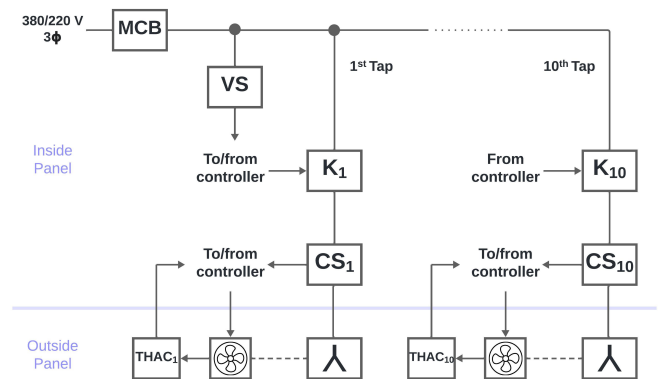


Figure 1. Single-line diagram of the bank's power circuit, along with protection and measurement devices. (MCB = Circuit Breaker;  $K_n$  =  $n^{th}$  Contactor;  $CS_n$  =  $n^{th}$  Current Sensor;  $Thac_n$  =  $n^{th}$  Thacometer; VS = Voltage Sensor;  $Y$  = Wye-Connected Load)

The load taps are wye-connected with 3 wires, and each branch is comprised of three series-connected heating elements. Thus, each element is subjected to 220/3 V, or 73.33 V; since their nominal voltage is 127 V, they only dissipate 333 W each, one third of its nominal power. As explained on Esther et al. (2020), this is intended to extend their lifespan.

Each tap is switched by a 25 A three-phase contactor, whose coil is energized at 220  $V_{ac}$ . The contactor includes a normally open (NO) contact pair that can provide feedback to the controller as to the state of the switch. 5 V relay modules with optocouplers provide the necessary electrical isolation and power amplification to allow the microcontroller's output ports to drive the cooling fans and contactor coils.

One voltage sensor board measures the three line voltages present in the bus; each tap will include an individual three-phase current sensor.

### 2.3 Construction

The load bank is designed to be built on a rolling cart, allowing easy mobility. Each load tap, along with its cooling fan is fitted in a slot, in order to provide air flow to each set of resistors without obstruction. The bank's control panel will also be mounted on the cart, and contain all the sensor boards, contactors, main circuit breaker, system controller and CAN bus adapter module. Figure 2 shows the conceptual design of the complete bank.

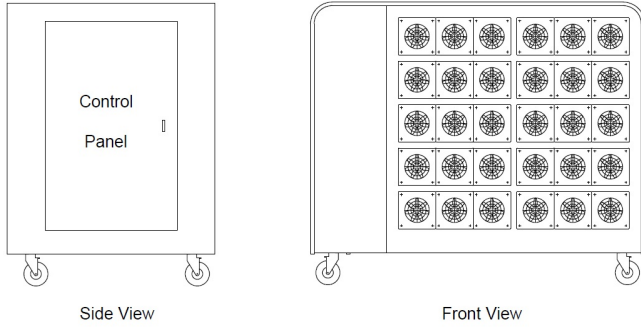


Figure 2. Conceptualized view of the assembled load bank.

The heating elements of each three-phase tap are mounted inside ventilation ducts, made out of sections of polyvinyl chloride (PVC) pipe. They are contained in an medium-density fiberboard (MDF) package (Figure 3), that can be attached to or removed from the cart in a modular fashion, facilitating maintenance.

Each duct (Figure 3) contains the three resistive elements that make up one phase of the load.

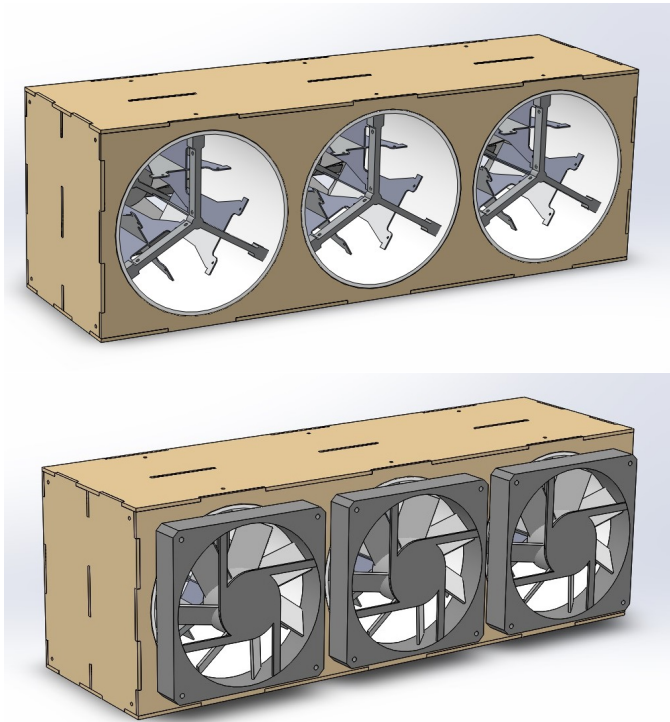


Figure 3. Top: front view of a duct package in *SolidWorks*<sup>®</sup>. Bottom: back view showing cooling fans.

These elements are evenly spaced inside the duct, at equal distances from the fan, in order to provide uniform cooling;

opposed to what was proposed on Esther et al. (2020), where it is suggested the heating elements be arranged in series. In such arrangement the elements furthest away from the fan become much hotter than those close to it. The resistor elements with a conical shape are positioned with the smaller-diameter end close to the fan, and the bigger-diameter end close to the free opening of the duct (see Figure 3). Cooling is more efficient in this arrangement.

### 2.4 Sensors

Low-cost commercial circuits for voltage measurement generally operate at grid level voltage. Since the bank is designed to measure three-phase 380/220 V, a voltage sensor board was designed for this project. The voltage sensor sends the root mean square (RMS) value of the three line voltages to the system controller. The purpose of the sensor is to allow the user to monitor the voltage through the supervisory program, and verify it is within safe levels. Its approach is different to what was presented on Esther et al. (2020), as it extracts the peak value of the waveform.

The sensor operates with a ZMPT101B instrument transformer that provides an isolation voltage of 3 kV, and includes six 3 W input resistors, which were selected due to their larger size, in order to avoid potential sparking. The next stages include a voltage limiting diode bridge, a precision rectifier (Sedra and Smith, 2015) with filtering capacitor and discharge transistor, and a non-inverting amplifier that gives a final output-to-input ratio of:

$$V_{out} [V] = 0.01V_{in} [V_{rms}] \quad (1)$$

A 5.1-V zener diode protects the microcontroller's input port against overvoltage. Figure 4 (top) shows the circuit for a single phase.

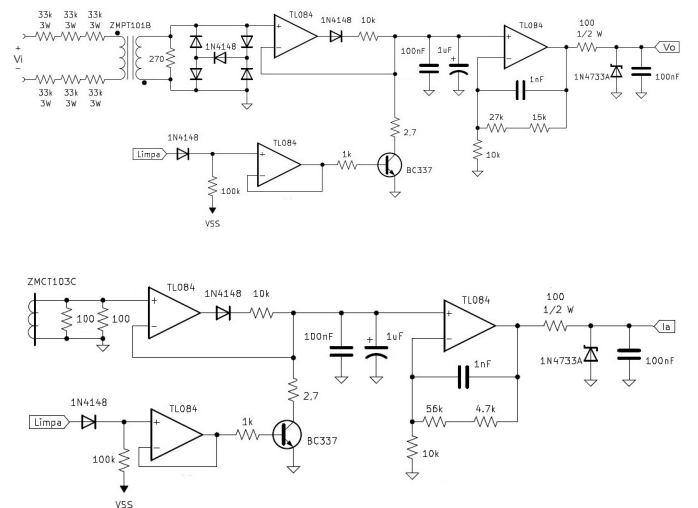


Figure 4. Circuit schematics for the voltage sensor (top) and current sensor (bottom).

In contrast to the original proposed system (Esther et al., 2020), current measurement is done on all three phases, and the sensor is no longer based on an ACS712-20A integrated circuit (IC). It has a very similar topology to the voltage sensor, except that employs a ZMCT103C

current transformer, as can be seen in Figure 4 (bottom). It presents an output-to-input ratio of 0.5 V/A.

It was decided not to measure the temperature of the heating elements directly on operation. Rather, the micro-controller reads the pulses from the cooling fans' built-in tachometers. If the fan speeds in a given tap are too low, it will deem that tap unavailable until repair.

### 3. CONTROLLER

#### 3.1 Implementation and Programming

The selected controller was an *Arduino Mega 2560* micro-controller board. It implements the tap rotation scheme described by Esther et al. (2020). To develop the controller's programming, a Real-Time Operating System (RTOS) was used, in particular, the *FreeRTOS*<sup>™</sup> library (Real Time Engineers Ltd, 2022).

The application developed in *FreeRTOS*<sup>™</sup> divides, among multiple threads of execution, the following tasks: i) receive commands from and send readings to the supervisory program, ii) register tap usage times, iii) switch taps according to their usage times and iv) read each one of the sensors and take action if a fault is suspected. As can be seen in Figure 5, these separate routines constantly exchange information through the use of flag bits, called *event groups* in *FreeRTOS*<sup>™</sup> terminology, and *queues*, which serve as buffers for measurements and commands.

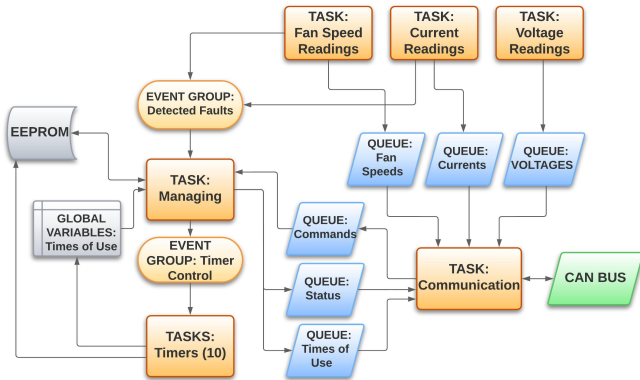


Figure 5. Structural diagram of the *FreeRTOS*<sup>™</sup> application.

#### 3.2 Communication

As introduced in Subsection 2.1, the system employs a CAN bus for communication. Since the *Arduino* board does not have the needed hardware to access the CAN bus directly, it was connected to a CAN BUS MCP2515 TJA1050 module; it can convert bytes coming from the *Arduino* into CAN messages, and vice versa. On the other side of the bus, a second identical module, paired with another *Arduino* board, couples the bus to a computer's universal serial bus (USB) port, so that the bytes can be read by the supervisory program. In operation, the CAN bus is transparent to both ends, which seem to be communicating directly through the serial port.

#### 3.3 User Interface

A user interface was developed to allow monitoring of the load bank's internal workings in real time, so that the user can read the data coming from the sensors and check the status of each load tap, in addition to being able to send load requests and block or unblock each tap individually. Its user interface was developed in the *Windows Forms* format and is show in Figure 6.

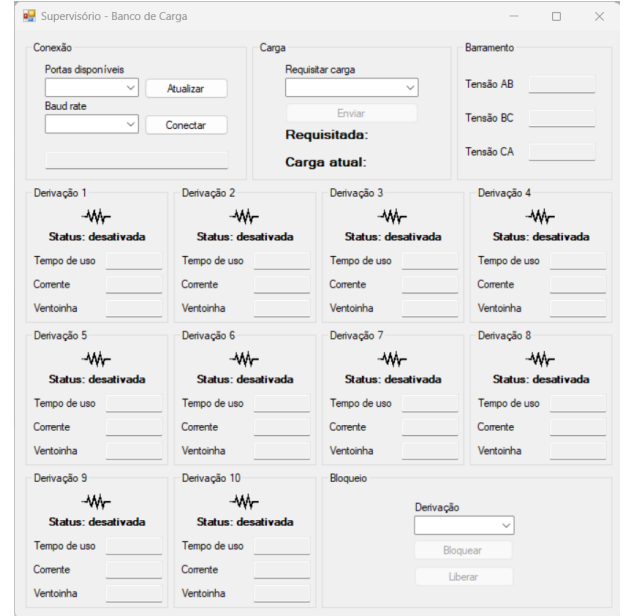


Figure 6. User interface of the supervisory program.

### 4. RESULTS

As discussed before, it is desirable for the load bank to be able to operate safely and reliably. Tests were performed on the proposed sensors, as well as thermal response tests, to make sure the temperature of the heating elements stays under safe limits.

In order to validate the proposed circuit for voltage measurement, a prototype was assembled on a breadboard, and tests were carried out to trace its response curve. A variable voltage was applied to its input, from 0 V to 540 V. Two multimeters measured the voltage at the input and output of the sensor.

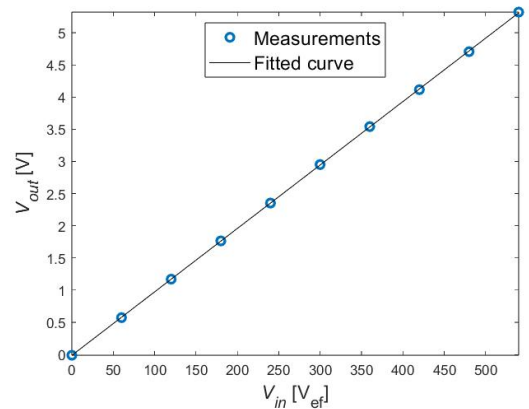


Figure 7. Voltage sensor prototype's response curve.

Ten input values were arbitrated, in steps of 60 V, and the corresponding output values were recorded. Measurements are presented in Figure 7, along with the line that best fits the values.

The fitted line is described by (2):

$$V_{out} [V] = -0.0121 + 0.0099V_{in} [V_{rms}] \quad (2)$$

which is very close to (1). Similar results were obtained for the current sensor. Two printed circuit boards were then built to measure all three phases (Figure 8).

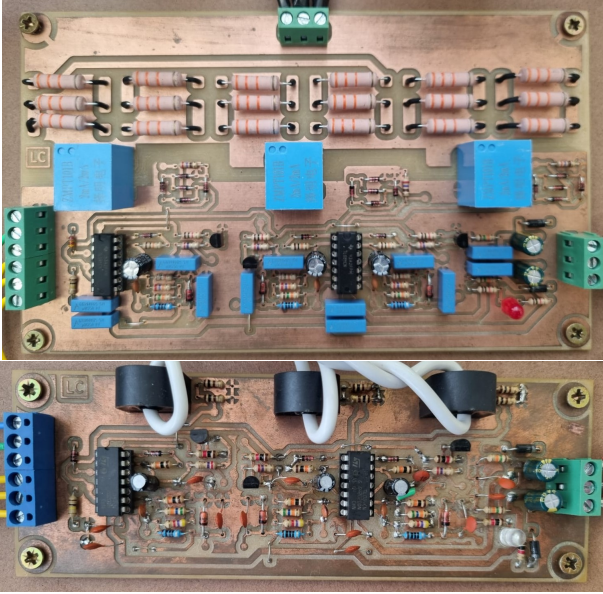


Figure 8. Voltage (top) and current (bottom) sensor boards.

A single load tap module was built according to the computer model (Figure 3), and a control panel prototype was built, including sensor boards, circuit breaker, contactor, microcontroller and relay module (Figure 9).

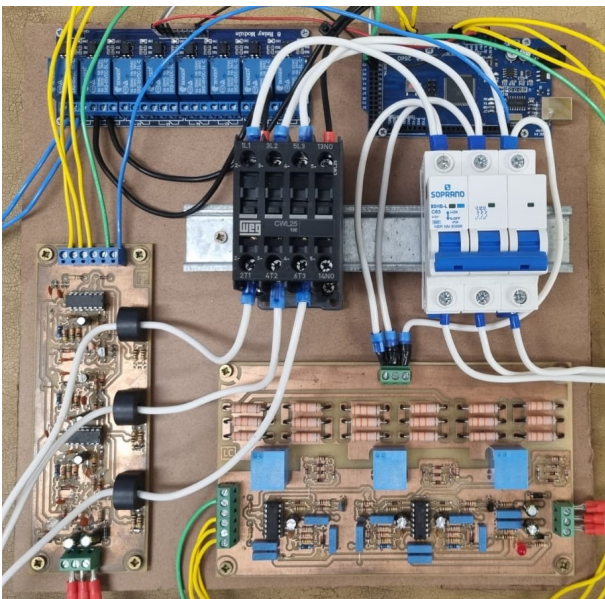


Figure 9. Control panel prototype for a single load tap.

As can be seen in Figure 10, the load module was assembled together with the control panel, and the *Arduino* was connected to a computer's serial port.

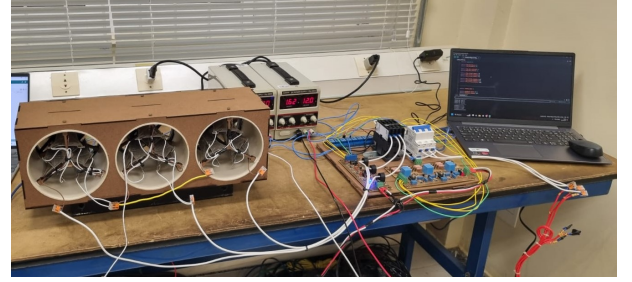


Figure 10. Load tap test assembly.

The load was supplied by the available 440/254 V source, higher than nominal values on Table 1. However, if it behaves appropriately it is assumed to do so under nominal conditions.

In order to acquire the load's thermal response, a thermocouple in contact with the heating wire was employed, as far away from the fans as possible. It won't be present in final design, the goal was to be sure the heating wires remain under safe temperature limits, provided the cooling fans are healthy and operational.

In each test, the load was turned on from room temperature (27 °C) and allowed to reach steady state, in a 60-second time window. The results were averaged from three different readings. The steady state values are compiled in Table 2; it shows the measured values are very close to what was expected.

Table 2. Steady State Test Results

Parameter	Phase A	Phase B	Phase C
Phase Voltage	244.80 V	246.18 V	243.42 V
Phase Current	5.44 A	5.43 A	5.49 A
Power per Phase	1332.5 W	1338.0 W	1335.5 W
Resistance at 27 °C	43.7 Ω	44.1 Ω	43.5 Ω
Resistance in Operation	44.98 Ω	45.30 Ω	44.37 Ω
Heating Element Temp.	108.82 °C	104.78 °C	114.48 °C
<b>Total Power</b>	<b>4005.9 W</b>		

Figure 11 shows how temperature evolved for each phase, with cooling fans at full speed. The total power consumption of the module can be seen on the same plot.

Sampled data were used to model the relation between the increase in temperature (in °C) and input power (in W) in each phase by the first order transfer function described below:

$$\frac{\Delta T(s)}{P(s)} = \frac{0.02316}{s + 0.3645} \text{ °C/W} \quad (3)$$

which yields a time constant of  $\tau = 2,74$  s. Several tests were performed, and although steady state temperatures differed depending on the position of the thermocouple, time constants remained the same.

Using sampled values of currents and voltages, wire resistances were calculated along the tests. As can be seen in Figure 12, the values on each phase are nearly identical, which means the load is well balanced. Furthermore, they barely changed with an increase in temperature from 27

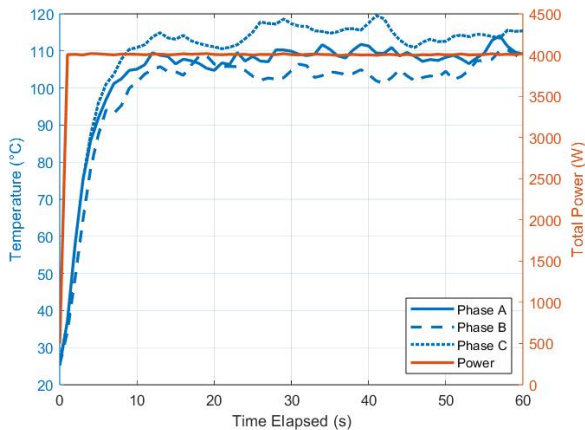


Figure 11. Three-phase dissipated power and thermal response for each phase after startup.

°C to about 100 °C, as expected from metal alloys used in heating wires (Powell, 1936).

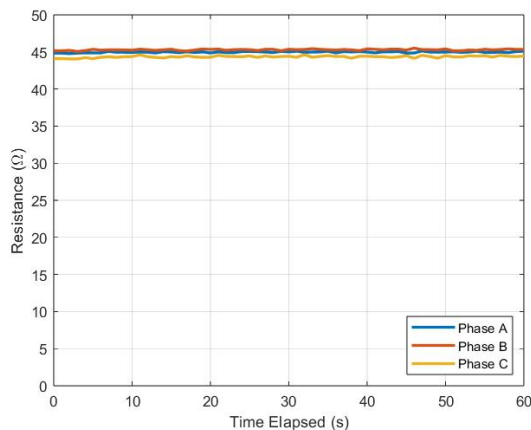


Figure 12. Resistance values for each phase after startup.

## 5. CONCLUSIONS

Results show the system behaves as expected and the microcontroller was able to sample the variables. On testing the load was powered at a voltage higher than its design value, dissipating more heat than it would in nominal condition. However, heating wire temperature remained under safe limits, ensuring safety and reliability. Those results for a single load tap enable a future full-scale assembly of the bank.

The total estimated cost is about R\$18,000.00. Commercial load banks aren't widespread in Brazilian local market, an imported 30 kW device price is well above R\$20,000.00, considering shipping and taxes. The device presented also employs readily available components, which facilitates maintenance and repair. It is suitable for being used in academic environments.

The heating wires are a passive element and their power demand depends on applied voltage. In addition, the load can only be applied in discrete steps, which allows studying the steady state performance of the hybrid-electric power-train, but it is not smooth enough to properly emulate the dynamic behaviour in transient response of a mechanical load on an axis such as a propeller.

Future research will develop a closed loop control strategy for maintaining power demand at a desired value in spite of voltage fluctuations, as well as allowing each load tap to operate at partial power. Thermal behaviour of the full bank, accounting for all load taps operating adjacent to each other, will also be studied.

## REFERENCES

- Bearn, P. (2012). Specifying, applying load-bank systems. **Consulting-Specifying Engineer**. URL <https://www.csemag.com/articles/specifying-applying-load-bank-systems/>. Accessed in: 01/09/2020.
- Celis Quintero, M., Hernandez Acosta, G., and Duarte Forero, J.E. (2020). Implementation of a 3.5 kw resistive load bank for a single-cylinder diesel engine test bench. *Scientia et Technica*, 25(4), 598–505.
- Esther, D.M., de Almeida Fernandes, D., and Rendón, M.A. (2020). Banco de carga trifásico resistivo inteligente de 35kw de baixo custo. *Anais do XXIII Congresso Brasileiro de Automática*, 2(1), 1104.
- Jackson, A. et al. (2021). A modular multi-phase actively controlled resistive load bank with zero-current switching capability and integrated snubbers. In *2021 IEEE Power and Energy Conference at Illinois (PECI)*, 1–6. IEEE.
- Kehler, L.B. et al. (2013). Electronically adjustable load for testing three phase ac systems. In *2013 Brazilian Power Electronics Conference*, 1082–1087. doi:10.1109/COBEP.2013.6785249.
- Powell, R.W. (1936). The thermal and electrical conductivities of metals and alloys: Part 2, some heat-resistant alloys from 0°C to 800°C. *Proceedings of Physical Society*, 48(3), 381–392.
- Prapurt, N. and Lothongkam, C. (2022). Design and development of the 20 kw load bank set for performance testing of standby generators. In *2022 25th International Conference on Electrical Machines and Systems (ICEMS)*, 1–5. doi:10.1109/ICEMS56177.2022.9982929.
- Raj, R., Vishnukumar, T.S., and Murugan, R. (2023). Automating load banks for enhanced testing efficiency. *3rd International Conference on Emerging Frontiers in Electrical and Electronic Technologies (ICEFEET)*.
- Real Time Engineers Ltd (2022). **FreeRTOS**. Front page. URL <https://www.freertos.org/index.html>. Accessed in: 18/08/2022.
- Sedra, A.S. and Smith, K.C. (2015). *Microeletrônica*. Pearson Makron Books, São Paulo, SP, 7<sup>th</sup> edition.
- Sepasi, S. et al. (2023). A practical solution for excess energy management in a diesel-backed microgrid with high renewable penetration. *Renewable Energy*, 202.
- Simplex (2020). Load bank fundamentals. **Simplex Direct**. URL <https://www.simplexdirect.com/loadbanksEducation.aspx>. Accessed in: 01/09/2020.
- Worldwide Power Products (2020). Load bank types: resistive vs reactive vs resistive/reactive vs electronic. **W Power Products**. URL <https://www.wpowerproducts.com/news/load-bank-types/>. Accessed in: 01/09/2020.